Reactivity of BrNO 2 and ClNO 2 with Solid Alkali Salt Substrates

ARTICLE *in* THE JOURNAL OF PHYSICAL CHEMISTRY A · SEPTEMBER 1998

Impact Factor: 2.69 · DOI: 10.1021/jp982000f

Reactivity of $BrNO_2$ and $ClNO_2$ with Solid Alkali Salt Substrates

François Caloz,† Sabine Seisel, Frederick F. Fenter, and Michel J. Rossi*

Laboratoire de Pollution Atmosphérique et Sol (LPAS), Swiss Federal Institute of Technology (EPFL), 1015 Lausanne, Switzerland

Received: April 27, 1998; In Final Form: June 23, 1998

The reactions of $BrNO_2$ and $ClNO_2$ with bromide have been studied in a Knudsen-cell reactor in order to better understand the elementary reactions of these potentially important tropospheric species in the presence of solid sea-salt aerosol. $BrNO_2$ efficiently reacts with bromide to produce molecular bromine ($\gamma > 0.3$). To better understand the fate of $BrNO_2$ in the Knudsen-cell reactor, we have developed a $BrNO_2$ source based on the reaction of molecular bromine with solid KNO_2. We have determined that the lifetime of $BrNO_2$ under our experimental conditions is on the order of 10 s and is limited by heterogeneous decomposition reactions. The interaction of $BrNO_2$ with KBr, KCl, and KNO_2 was studied using the external $BrNO_2$ source. $ClNO_2$ can be converted to $BrNO_2$ in the presence of solid bromide, characterized by an uptake probability of $\gamma = 1.3 \times 10^{-4}$, in good agreement with results obtained for several substrate presentations such as salt powder, grain, and single crystals. We compared these results with previous work and briefly discuss atmospheric implications.

Introduction

It has been well established that N_2O_5 can react with salt to produce volatile nitryl halides of the type $X-NO_2$ [1−7] in what appears to be a displacement reaction:

$$N_2O_5 + NaCl \rightarrow ClNO_2 + NaNO_3 \quad (1)$$

$$N_2O_5 + KBr \rightarrow BrNO_2 + KNO_3 \quad (2)$$

The presence of these compounds may have an important impact on the oxidizing potential of the Earth's troposphere, as they represent activated halogen compounds which may release a halogen atom upon photolysis. Although bromide is a small fraction of sea salt ($[Cl^-]/[Br^-]$ is approximately 600/1), there is growing evidence that catalytic reactions are responsible for the importance of atmospheric bromine chemistry. Because of the potential role of reactions 1 and 2 in the atmosphere, we have investigated the fate of the product species $BrNO_2$ and $ClNO_2$ in the presence of salt surfaces using a low-pressure Knudsen reactor which is part of a flowing gas experiment.

An important goal of this kinetic study is to characterize the behavior of the key intermediate, $BrNO_2$, under our typical experimental conditions in light of earlier work carried out on this reaction system in previous laboratory studies.[1,8] In particular, we have shown in previous work that the only observed stable gas-phase product of reaction 2 under our conditions is molecular bromine. This result is in disagreement with work performed in other laboratories, where direct evidence for the presence of $BrNO_2$ has been obtained.[8] We postulated that $BrNO_2$ is formed as a primary product, which however remained undetectable under our experimental conditions due to its reactivity with bromide:

$$BrNO_2 + KBr \rightarrow Br_2 + KNO_2 \quad (3)$$

The enthalpy of reaction $\Delta H_r^0{}_{298} = -16.2$ kJ mol^{-1} of reaction 3 has been estimated using the value for the heat of formation of $BrNO_2$ (71.1 ± 7.5 kJ mole^{-1}) given by Wine and co-workers.[9]

In addition, we will report our results on the reaction of $ClNO_2$ with bromide. $ClNO_2$ is not reactive toward chloride. Therefore the reaction with bromide is of interest not only because of its atmospheric importance, but also because it represents a second pathway for $BrNO_2$ generation inside our Knudsen-cell reactor:

$$ClNO_2 + KBr \rightarrow BrNO_2 + KCl \quad (4)$$

Reaction 4 ($\Delta H_r^0{}_{298} = 15.6$ kJ mol^{-1}) may represent a competitive pathway to $ClNO_2$ photolysis and may be efficient at volatilizing bromine during the night. Moreover, hydrolysis of $BrNO_2$ according to reaction 5 may represent an additional source of HONO in the marine atmosphere.

$$BrNO_2 + H_2O \rightarrow HONO + HOBr \quad (5)$$

For this study, we have developed an *alternative $BrNO_2$ source* which is essential for testing the various hypotheses concerning the reactivity of $BrNO_2$ under our experimental conditions. The source is based upon reaction 6:

$$Br_2 + KNO_2 \rightarrow BrNO_2 + KBr \quad (6)$$

Experimental Details

For this study, we used a Teflon-coated Knudsen reactor, recently described in detail.[10,11] Briefly, the reactor is a two-chamber reactor operated in the molecular flow regime (see Table 1), which allows one to isolate the reactive surface and to perform reaction ON/reaction OFF experiments. Because of the low partial pressure on the order of 10^{-3} mbar or less,

* Author to whom correspondence should be addressed.
† Current address: Jet Propulsion Laboratory, Chemical Kinetics and Photochemistry Group, 4800 Oak Grove Dr., Pasadena, CA 91109.

S1089-5639(98)02000-3 CCC: $15.00
Published on Web 08/25/1998

TABLE 1: Knudsen Cell Parameters

cell parameter	value
volume (V)	1830 cm^3
estimated surface area (total)	1300 cm^2
surface area (A_S, sample)	19.6 cm^2
number density range	$(1-1000) \times 10^{10}$ cm^{-3} [a]
surface collision frequency (Z_1A_S)[b]	$38.7 \times (T/M)^{1/2}$ s^{-1}
escape rate constant for the 1 mm aperture (k_{esc})[c]	$0.02 \times (T/M)^{1/2}$ s^{-1}
escape rate constant for the 4 mm aperture[c]	$0.22 \times (T/M)^{1/2}$ s^{-1}
escape rate constant for the 8 mm aperture[c]	$0.80 \times (T/M)^{1/2}$ s^{-1}
escape rate constant for the 9 mm aperture[c]	$1.03 \times (T/M)^{1/2}$ s^{-1}
escape rate constant for the 14 mm aperture[c]	$1.77 \times (T/M)^{1/2}$ s^{-1}

[a] Calculated using the relation $F^i = Vk_{esc}[M]$, where F^i is the flow of molecules, V is the reactor volume, and [M] the number density. [b] Calculated for a sample surface of 19.6 cm^2. [c] Determined directly by experiment.

gas−wall collisions are favored over gas−gas collisions in the Knudsen reactor, making it well-suited for the study of heterogeneous processes. The different kinetic parameters which are necessary in order to use a Knudsen cell may be determined using simple gas kinetic expressions and are summarized in Table 2. The modulated effusive molecular beam leaving the Knudsen cell is analyzed by a quadrupole mass spectrometer (MS). The mass spectra of all observed compounds are listed in Table 3. In addition, the experiment was equipped with laser-induced fluorescence detection.[11] In the present work this technique was used to unambiguously detect NO_2 after excitation at 403 nm and broad band detection to the red of 500 nm using a photomultiplier protected by a cutoff filter. The signal acquisition was performed using a boxcar integrator (delay 9 μs, width 10 ns, average 30 pulses) resulting in a detection limit of 1×10^9 molecule/cm^3.

The gas-phase reactants are introduced into the Knudsen cell either through a glass capillary inlet or via a pulsed solenoid valve allowing the introduction of millisecond pulses. Dependent on the method of introducing the test gas, two different types of experiments referred to as *steady-state* and *pulsed-valve* experiments are routinely performed. Steady-state experiments are performed by introducing into the reactor a constant flow of molecules. By analysis of the change of the MS signal levels of the corresponding compounds upon opening and closing the sample chamber, a value for the net uptake coefficient γ may be calculated. Pulsed-valve, thus real-time, experiments have been performed by introducing a pulse of the test gas into the reactor. A reference pulse is introduced while the reactive surface is still isolated from the reactor volume. The rate constant for effusive loss k_{esc} is determined by simple fitting of an exponential decay function to the experimental MS signal trace in the absence of reaction. Repeating the same process with the plunger lifted, thus with the sample exposed, a reactive pulse is obtained. The observed single-exponential decay in the presence of a reactive surface is characterized by a new rate constant, k_{dec}, defined by $k_{dec} = k_{reac} + k_{esc}$.

The gas densities were determined in mass flow calibrations. The flow rate into the Knudsen reactor was measured by recording the pressure change as a function of time in a calibrated volume behind the capillary while monitoring the corresponding MS signal. The flow of molecules may then be related to the concentration of the gas molecules in the reactor. The HONO calibration has been performed in situ by reacting a known flow of HCl with solid $NaNO_2$ in the Knudsen cell. Using the observation that the reaction yield of HCl with $NaNO_2$ is 90% to result in HONO, the loss of the HCl MS signal may be quantitatively related to HONO (m/e 47).

In this work we have synthesized $ClNO_2$ according to the procedure proposed by Ganske and co-workers.[12] Briefly, pure HCl gas is passed through a mixture of fuming nitric and sulfuric acid, and the evolving gases are collected in a liquid nitrogen cooled trap. The obtained product mixture is then twice distilled to eliminate molecular chlorine and nitric acid. The purity of the synthesized $ClNO_2$ has been checked by MS. No Cl_2 (m/e 70) and no HNO_3 (m/e 63) have been observed.

To differentiate between the various potential sinks of $BrNO_2$ in our reactor, both gas-phase and heterogeneous, it is necessary to rely on a source of $BrNO_2$ other than the in-situ reactions 2 and 4. In this work we developed a $BrNO_2$ source appropriate for a low-pressure reactor, based on reaction 6. The design of the source is schematically presented in Figure 1, where we show a second Knudsen cell mounted upstream to the reactor and containing solid granular KNO_2. Molecular bromine is passed through the source reactor in order to produce $BrNO_2$ via reaction 6. Two parameters are important for the source design: (1) The escape rate constant of the source Knudsen cell has to be as large as possible (>5 s^{-1}) in order to minimize the residence time of $BrNO_2$ in the source reactor, and (2) the orifice of the source reactor has to be as small as possible in order to avoid back-diffusion of $BrNO_2$ from the main reactor; i.e., the volume of the source reactor has to be small compared to that of the main reactor. The chosen source reactor geometry was a cylinder of 6 cm height and 4 cm diameter with an escape orifice diameter of 8 mm. According to the equations presented in Table 2, and using a value for the uptake coefficient for reaction 6 of 0.32 (see below), the source is able to convert 90% of the molecular bromine at a residence time for $BrNO_2$ in the source reactor of less than 1 s. In addition to $BrNO_2$, the major emitted gases were Br_2 and NO_2 in a ratio of approximately 1:10.

To take into consideration diffusion[13] of the gas molecules into the bulk of the salt under our experimental conditions we have used different types of surfaces: bulk salt powders, sieved grain substrates having grain diameters between 300 and 400 μm, spray deposited surfaces, and single-crystal optical salt flats, the two latter without internal surface. Before each experiment, the fresh salt surface has been held under vacuum for several hours in order to desorb the adsorbed surface water. Occasionally, the salt samples were heated under vacuum to 500 K to completely eliminate adsorbed water. Single-crystal optical flats have been treated in two different ways, referred to as *polished* and *depolished*. Polished surfaces are prepared by gliding a sheet of wet optical paper over the surface and then allowing it to dry. The salt flats are depolished by gentle rubbing using fine-grained sandpaper with careful subsequent elimination of the powder generated at the surface. All salts are commercially available: Fluka NaCl p.a., KNO_2 p.a., KBr p.a., $NaNO_3$ MicroSelect, KCl MicroSelect. The various kinds of surface preparation have been described in detail in previous work.[1,14]

Results

To study the reactivity of $BrNO_2$ toward various salts we had to develop an appropriate $BrNO_2$ source. As already described in Experimental Details, the source is based on the reaction of Br_2 with KNO_2 (reaction 6). We begin this section with a presentation of our results of a study of reaction 6 because these data provide the needed information on the $BrNO_2$ lifetime and reactivity characterizing our source.

TABLE 2: Relevant Equations

number	equation	note
1	$Z_1 = (8RT/\pi M)^{0.5}(1/4V)$	Gas−wall collision frequency (molecule^{-1} cm^{-2}). V is the volume of the reactor (cm^3).
2	$k_{esc} = Z_1 A_H$	Escape rate constant (s^{-1}). A_H is the escape orifice surface area (cm^2).
3	$k_{uni} = k_{esc}\,(S_0/S_R - 1)$	First-order rate constant for the uptake (s^{-1}). S_0 and S_R refer to the MS signals measured before and during reaction.
4	$\gamma = k_{uni}/(Z_1 A_S)$	Uptake coefficient. A_S refers to the geometrical area of the sample surface.
5	$P = RTF^i/k_{esc}\,V$	Vapor pressure determined in the steady-state experiment described in the text.

TABLE 3: Mass Spectral Data

species	parent peak[a]	fragment[a]	fragment[a]	fragment[a]	fragment[a]
$BrNO_2$		*93*, 95 (1)	46 (100)	30 (80)	79, 81 (10)
$ClNO_2$		*49* (1)	46 (100)	30 (50)	35 (10)
Br_2	*160* (100)	79, 81 (17)			
NO_2	*46* (50)	30 (100)			
HONO	*47* (12)	30 (100)			

[a] Ion mass with peak intensity in parentheses, given as percent of the most intense peak. The numbers in italics indicate the mass fragments which were used to monitor the species by MS.

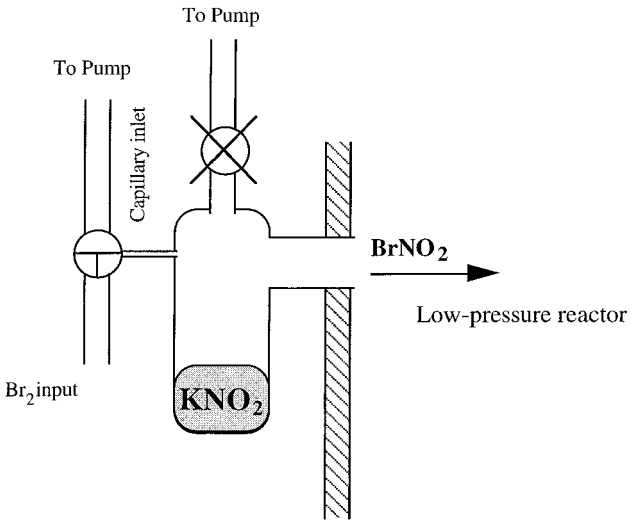

Figure 1. Schematic drawing of the external source of $BrNO_2$. The source is a small Knudsen cell containing nitrite and mounted directly on the main reactor. Molecular bromine is introduced through a capillary or a needle valve.

TABLE 4: Results on Reaction $Br_2 + KNO_2$

substrate	expt type	uptake coeff	no. of expts
powder	steady-state	0.32 ± 0.03	10
powder	pulsed-valve	0.28 ± 0.05	2
spray sample	steady-state	0.36 ± 0.05	2
spray sample	pulsed-valve	0.3 ± 0.1	1
		av 0.32 ± 0.05	

$Br_2 + KNO_2$: A Source Reaction for $BrNO_2$. *Kinetics of Reaction 6.* Reaction 6 has been measured to be fast with an uptake coefficient of $\gamma = 0.32 \pm 0.05$. This value has been found to be independent of reactant density and of sample surface presentation (see Table 4). We therefore conclude that reaction 6 is a first-order process. The independence of the results on the surface presentation is in agreement with the model of surface diffusion proposed by Keyser and co-workers[13] which does not predict any significant changes in the observed uptake coefficient for the case of large uptake rates. This case may be compared to the interaction of $ClONO_2$ with salt surfaces that has been studied previously.[14]

Product Analysis. Initial experiments were conducted using the Knudsen-cell reactor in the steady-state configuration, in which a constant flow of molecular bromine [$(1-10) \times 10^{14}$ molecules s^{-1}] was allowed to react with KNO_2. These experiments showed a large uptake rate of Br_2 (detected at *m*/*e* 160) and the appearance of new signals at *m*/*e* 30 (NO^+), 46 (NO_2^+), and 93 and 95 (BrN^+), as shown in Figures 2 and 3. The product mass spectrum indicates the presence of $BrNO_2$. When the gas-phase residence time in the Knudsen reactor is increased by reducing the exit-orifice diameter from 14 mm to 1 mm, the ratio *m*/*e* 30 to 46 increases (see Figure 3). This suggests that secondary products are formed which have a strong contribution at *m*/*e* 30 (NO^+). Possible candidates are BrNO, HONO, NO_2, and NO. BrNO and HONO both have strong parent-ion signals at *m*/*e* 109, 111 and at *m*/*e* 47, respectively, and thus can be unambiguously monitored by MS. In ancillary experiments on reaction 6, we investigated the formation of these possible secondary products which may contribute to mass 30 (NO^+). BrNO was not detected (*m*/*e* 109 and 111), but we did observe slow HONO production (*m*/*e* 47), as shown in Figure 4. We attribute this to the hydrolysis reaction of $BrNO_2$ (reaction 5).

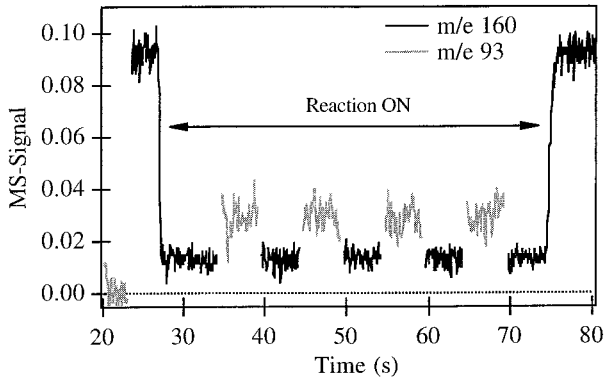

Figure 2. Steady-state experiment on the reaction of $Br_2 + KNO_2$ (reaction 6) performed using the 14 mm orifice with a Br_2 flow of 3.8×10^{14} molecules s^{-1}. During this experiment we monitored the MS signal at *m*/*e* 93 (BrN^+) and at *m*/*e* 160 (Br_2^+).

The yield of HONO is 10% with respect to Br_2 taken up on samples that were dried under vacuum without heating. Thus, when we take into account reaction 6 under our experimental conditions, only 10% of the $BrNO_2$ undergoes hydrolysis. HOBr, however, was not detected because it undergoes a fast reaction with KBr according to reaction 7:

$$HOBr + KBr \rightarrow Br_2 + KOH \qquad (7)$$

Reaction 7 has recently been studied in our laboratory and shown to be fast ($\gamma > 0.1$), and molecular bromine was detected as a product.[15] HONO disappeared from the product mass spectrum of reaction 6 when the salt sample was dried under vacuum in the Knudsen reactor by heating it to 500 K using a high-temperature sample support.

We concluded that the product mass spectrum of reaction 6 was consistent with the presence of large amounts of NO_2. To simplify the analysis of the NO_2 yield, it was necessary to conduct experiments using LIF detection of NO_2. These LIF experiments were performed at an excitation wavelength of 403

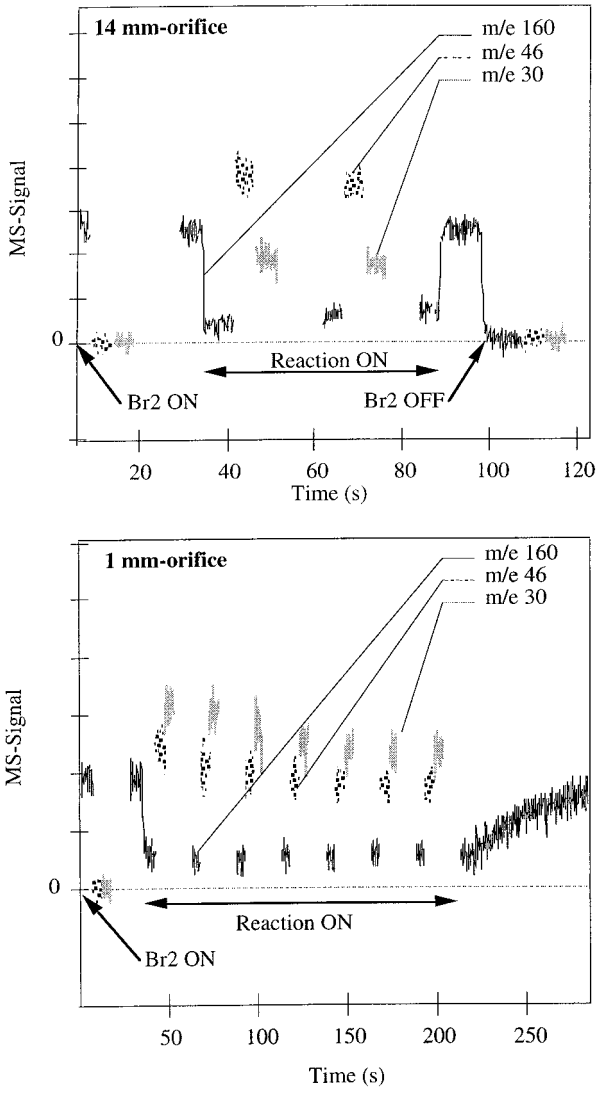

Figure 3. This figure displays two steady-state experiments on the reaction of $Br_2 + KNO_2$ (reaction 6) performed using two different orifice sizes and a molecular bromine flow rate of 4.5×10^{14} molecules s^{-1}. The residence time of $BrNO_2$ in the reactor is varied by about 2 orders of magnitude. Note the variations in the ratio of the recorded signals at mass *m*/*e* 46 and *m*/*e* 30 which decreases with decreasing orifice size.

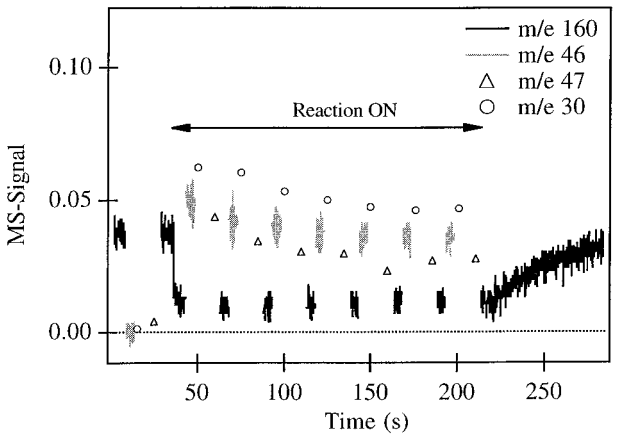

Figure 4. The steady-state experiment on the reaction of $Br_2 + KNO_2$ (reaction 6) presented in this figure has been performed using a Br_2 flow of 4.5×10^{14} molecules s^{-1} and the 1 mm orifice. HONO and Br_2 are detected at *m*/*e* 47 and *m*/*e* 160, respectively, during the reaction.

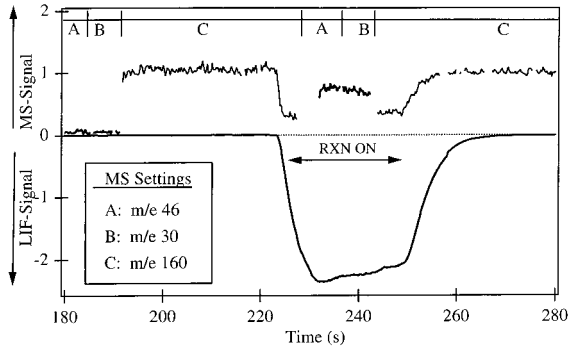

Figure 5. Typical signals obtained during a combined LIF/MS experiment on the reaction of $Br_2 + KNO_2$ (reaction 6). This experiment was performed using the 4 mm orifice at a Br_2 flow rate of 5.3×10^{14} molecules s^{-1}. The sample chamber was opened after 220 s and closed after 250 s. The LIF signal is displayed here as a negative-going signal. During this experiment we have measured a NO_2 yield of 0.89 per molecular bromine taken up.

TABLE 5: Results of LIF Experiments of the Reaction $Br_2 + KNO_2$

orifice [mm]	k_{esc} [s^{-1}]	t_{res} [s]	NO_2 yield[a]	*m*/*e* 46[b]	*m*/*e* 30[b]
14	3.1	0.32	25 ± 10%	1	0.85 ± 0.05
9	1.7	0.6	40 ± 10%	1	0.85 ± 0.05
8	1.33	0.8	50 ± 20%	1	0.85 ± 0.05
4	0.33	3	90 ± 20%	1	1.0 ± 0.3
3	0.19	5.3	95 ± 20%	1	1.0 ± 0.3
2.3	0.11	9.1	130 ± 30%		
1	0.03	33	200 ± 50%		

[a] NO_2 yield per Br_2 lost through reaction. [b] Normalized residual MS signal after subtraction of the NO_2 contribution. The values for the two smallest orifices are not given because the residual is too small.

nm, and an example is shown in Figure 5. The results are summarized in Table 5. The NO_2 yield with respect to the consumption of Br_2 increases with increasing residence time and reaches 200% when using the smallest escape orifice (residence time of approximately 25 s). To interpret these results, we propose the following reaction mechanism:

$$Br_2 + KNO_2 \rightarrow BrNO_2\,(ads) + KBr \qquad (6)$$

$$BrNO_2\,(ads) \rightarrow 1/2\ Br_2 + NO_2 \qquad (8)$$

$$1/2\ Br_2 + KNO_2 \rightarrow KBr + NO_2$$

We note that reaction 8 may not correspond to an elementary reaction. The most probable mechanism involves a fast heterogeneous recombination of atomic bromine yielding Br_2 (reaction 8a). We did not observe free bromine atoms under the same conditions where we have observed Br in the gas phase from the reaction of NO_3 free radical with KBr.[26] Therefore, we think that the recombination of Br follows a Langmuir−Hinshelwood mechanism displayed in reaction 8a.

$$2\ Br(ads) \rightarrow Br_2 \qquad (8a)$$

The observed mass spectrum for $BrNO_2$, after correction for the presence of NO_2, does not change significantly as a function of residence time (see Table 5), in support of this mechanism.

The radical product, NO_2, originates from the decomposition of $BrNO_2$. As discussed below, this decomposition (reaction 8) takes place on some uncoated parts of the internal surfaces of the reactor and has only a vanishingly small homogeneous gas-phase contribution. This step is strongly favored because the gas−wall interaction is predominant under the low-pressure

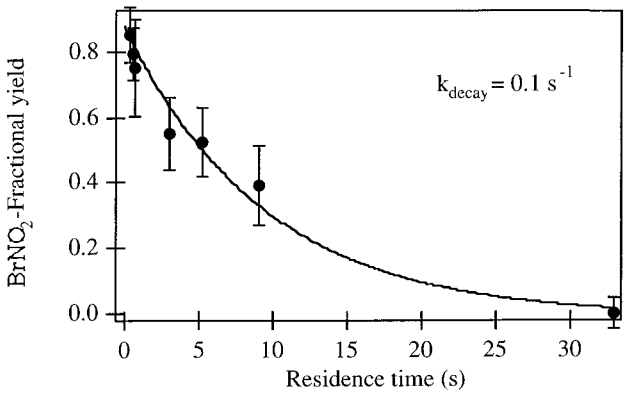

Figure 6. Display of the fractional yield of $BrNO_2$ as a function of the calculated gas-phase residence time of $BrNO_2$ in the Knudsen reactor. The solid line is a single-exponential fit.

conditions. According to the above scheme, reaction 8 produces molecular bromine and NO_2; thus, for each mole of Br_2 consumed in the reaction with KNO_2, 1 mol of NO_2 and 0.5 mol of Br_2 are produced, resulting in a 200% yield of NO_2 with respect to loss of Br_2.

Lifetime of $BrNO_2$ in the Knudsen Cell. Detailed analysis of the LIF experimental results on reaction 6 allows the determination of the lifetime of $BrNO_2$ in our reactor. At steady state, the flow of $BrNO_2$ molecules from the reactor is given by the consumption of the molecular bromine flow and by the production of nitrogen dioxide, according to

$$F^{o}(BrNO_2) = [F^{i}(Br_2) - F^{o}(Br_2)] - 0.5\,F^{o}(NO_2) \qquad \text{(E1)}$$

where the superscripts o and i represent the outgoing and incoming gas flows. The LIF signals, which correspond to a density measurement, have to be converted into equivalent flows for eq E1, using the relation $F^{o}(NO_2) = [NO_2]k_{esc}(NO_2)V$. In Figure 6 we have plotted the fractional yield, f, of $BrNO_2$ against residence time, whose variation was obtained by changing the escape orifice:

$$f = \frac{F^{o}(BrNO_2)}{F^{i}(Br_2) - F^{o}(Br_2)} \qquad \text{(E2)}$$

The solid line shown in the figure is an exponential fit that corresponds to a $BrNO_2$ lifetime of 10 s within our Knudsen-cell reactor. Additional experiments on the lifetime of $BrNO_2$ in our reactor have been performed using the external $BrNO_2$ source. A comparison of the MS signals at *m*/*e* 95 (BrN^+) at different residence times resulted in the same lifetime as determined above, supporting the heterogeneous decomposition mechanism proposed above.

In Table 5 we present the residual MS signal after subtraction of the NO_2 contribution for both *m*/*e* 46 and *m*/*e* 30, determined from a calibration of the LIF signal for NO_2. We point out that this residual MS signal corresponds to the sum of all possible reaction products except NO_2. This spectrum remains constant for different orifice sizes and therefore for different residence times, which is evidence for the presence of only one important product in the mixture, namely $BrNO_2$. The slight increase in the relative signal at *m*/*e* 30 at long residence times might be due to an additional contribution to this mass peak by HONO, but the uncertainties of the measurements and of the subtraction procedure (large numbers leading to a small residual) are large for long residence times. We conclude that the relative MS intensities for $BrNO_2$ resulting in a ratio of 0.85 for the MS intensities at *m*/*e* 30 and 46 have been determined in good accuracy from experiments displayed in the first three entries of Table 5. In ancillary experiments using the external $BrNO_2$ source, the complete MS spectrum has been determined to be 46 (100%), 30 (80%), 79 (10%), and 93, 95 (1%); here the relative intensities are given in parentheses and are found to be in agreement with the results presented above.

In conclusion, the uptake of Br_2 on KNO_2 is fast and produces $BrNO_2$ with a lifetime of 10 s in our reactor. Therefore the reaction is suitable as a source of $BrNO_2$.

Reactivity of $BrNO_2$. Once we had established an appropriate $BrNO_2$ source, we studied its reactivity on various salts. One disadvantage of this source is that an exact calibration of the MS signal of $BrNO_2$ is not available. Therefore the study is limited to the measurement of uptake coefficients and the identification of products.

$BrNO_2$ + $NaNO_3$. To obtain information on the heterogeneous decomposition of $BrNO_2$ on salt surfaces (reaction 8), we performed uptake experiments of $BrNO_2$ on $NaNO_3$. $NaNO_3$ is a non-halogen-containing salt. Thus, we are able to differentiate between the heterogeneous decomposition according to reaction 8 and the reaction with salt according to reaction 3. Steady-state experiments on the uptake of $BrNO_2$ on $NaNO_3$ powder have been performed in which $BrNO_2$ was monitored at *m*/*e* 95 using the external $BrNO_2$ source. We observed a weak interaction of $BrNO_2$ resulting in an uptake coefficient of $\gamma = 5 \times 10^{-3}$. No changes of either Br_2 or NO_2 have been observed in the gas phase, indicating that the interaction is nonreactive and that decomposition of $BrNO_2$ does not take place on $NaNO_3$ under the prevailing experimental conditions. This result asserts that products observed during the uptake of $BrNO_2$ on halogen-containing salt are due to the reaction of $BrNO_2$ on the alkali halide salt sample.

$BrNO_2$ + KBr. We have shown in ref 1 that $BrNO_2$, the primary product of reaction 2, remained undetectable under our experimental conditions. The only observed stable gas-phase products were molecular bromine and a small amount of HONO which was attributed to a secondary reaction (reaction 5). To explain these experimental results we postulated that $BrNO_2$ is highly reactive toward bromide (reaction 3). Using the external $BrNO_2$ source presented above, we were able to test this hypothesis. Steady-state experiments of the uptake of $BrNO_2$ on KBr powder substrates indeed obtained a fast rate of uptake of $BrNO_2$ on KBr with an uptake coefficient of $\gamma \geq 0.3$. The only detectable gas-phase product was molecular bromine, in agreement with reaction 3. No NO_2 formation has been observed using sensitive LIF detection, indicating that the reaction of $BrNO_2$ with bromide (reaction 3) is faster than its heterogeneous decomposition (reaction 8).

$BrNO_2$ + KNO_2. The assumption that two molecules of NO_2 are produced for each Br_2 molecule lost according to the sum of reactions 6 and 8 is the basis for the lifetime analysis carried out above. It is therefore necessary to investigate the potential NO_2 formation by the secondary reaction between $BrNO_2$ and nitrite (reaction 9), which results in the same net reaction and relative yields of NO_2 per Br_2 lost as the net of reactions 6 and 8 in order to assert that $BrNO_2$ in fact undergoes heterogeneous decomposition (reaction 8) releasing NO_2:

$$Br_2 + KNO_2 \rightarrow BrNO_2 + KBr \qquad (6)$$

$$BrNO_2 + KNO_2 \rightarrow 2\,NO_2 + KBr \qquad (9)$$

$$Br_2 + 2\,KNO_2 \rightarrow 2\,KBr + 2\,NO_2$$

We have performed steady-state experiments on the uptake of $BrNO_2$ on KNO_2 powder using the external $BrNO_2$ source. Since Br_2 is always emitted from the source and readily reacts with KNO_2 according to reaction 6, these experiments are difficult to interpret. In cases where higher Br_2 concentrations were present in the reactor an increase in the MS signal at *m*/*e* 93 has been observed, indicating formation of $BrNO_2$ according to reaction 6. At the same time, the formation of NO_2 has also been observed using LIF detection. However, at small levels of Br_2 ($F^i < 10^{14}$ molecules/s) emitted from the $BrNO_2$ source, we observed a weak interaction of $BrNO_2$ with KNO_2 accompanied by a decrease in the LIF signal of NO_2, indicating a decrease in the rate of formation of NO_2 according to reaction 8. Therefore, the uptake of $BrNO_2$ on KNO_2 is nonreactive, similar to the uptake on $NaNO_3$, and no NO_2 is formed. We conclude that reaction 9 is too slow under our experimental conditions so that the observed NO_2 results from the heterogeneous decomposition shown in reaction 8.

$BrNO_2$ + KCl. The interaction between $BrNO_2$ and KCl may produce two different products:

$$BrNO_2 + KCl \rightarrow ClNO_2 + KBr \qquad (10a)$$

$$BrNO_2 + KCl \rightarrow BrCl + KNO_2 \qquad (10b)$$

In steady-state experiments the initial uptake coefficient of $BrNO_2$ on KCl powder substrates monitored by MS at *m*/*e* 95 was measured as $\gamma = 5 \times 10^{-2}$. The $BrNO_2$ rate of uptake decreased with exposure time. A second exposure on the same salt sample, again of a length of approximately 1 min, already reduced the uptake coefficient by a factor of 2. No chlorine-containing gas-phase product was observed. The expected products of reaction 10a and 10b do not interact with KCl, an observation which has been verified in an ancillary experiment. This result is in disagreement with the work of Frenzel et al.[8] who observed the formation of $ClNO_2$ during the uptake of $BrNO_2$ on chloride solutions. The only gas-phase product we were able to detect was molecular bromine followed by MS at mass *m*/*e* 160. No formation of HONO has been observed which excluded the hydrolysis of $BrNO_2$ (reaction 5) followed by reaction 7 as a sink for $BrNO_2$. Since the $BrNO_2$ source does not allow one to establish a mass balance, it is unclear whether molecular bromine is formed by decomposition of $BrNO_2$ according to reaction 8 or by fast reaction of either $BrNO_2$ or BrCl[14] with impurities of bromide in the KCl sample (reaction 3). However, we have some indirect evidence for the occurrence of a secondary reaction: (i) $BrNO_2$ does not decompose on $NaNO_3$, and therefore efficient heterogeneous decomposition on the salt may be excluded; (ii) during the uptake of $BrNO_2$ on KCl, no formation of NO_2 following the heterogeneous decomposition (reaction 8) has been observed using LIF. This suggests that $BrNO_2$ reacts faster than it heterogeneously decomposes on the KCl salt surface according to reaction 8; (iii) the KCl sample contains 0.05% bromide as an impurity. Experiments on NaCl with a bromide content of 0.005% resulted in an initial uptake coefficient of $\gamma_0 = 2.2 \times 10^{-2}$, which is significantly smaller than the value obtained on the KCl sample. On the other hand, when the bromide content is increased to 2% the uptake of $BrNO_2$ increases to a initial value of $\gamma = 0.2$. At the same time a higher yield of Br_2 has been obtained. These facts, namely the correlation of both the initial uptake coefficient and the Br_2 yield with the bromide content of the salt, the saturation behavior of the uptake, and the absence of NO_2 formation let us conclude that $BrNO_2$ is reacting only with the bromide impurity of the salt and not with chloride itself.

TABLE 6: Results of LIF Experiments of the Reaction $ClNO_2 + KNO_2$ (Reaction 11)

orifice [mm]	τ ($ClNO_2$) [s]	γ ($ClNO_2$)	NO_2 yield[a]
14	0.3	1.8×10^{-2}	25%
8	0.7	1.7×10^{-2}	37%
4	2.4	1.5×10^{-2}	46%
1	26	5.4×10^{-3}	194%

[a] NO_2 yield per $ClNO_2$ lost through reaction.

TABLE 7: Br_2 and NO_2 Yields of Reactions 2 and 4

reaction	expt type	Br_2 yield[a]	NO_2 yield[b]
N_2O_5 + KBr (2)	steady-state	0.35 ± 0.05	
$ClNO_2$ + KBr (4)	steady-state	0.61 ± 0.22	0.2 ± 0.1
$ClNO_2$ + KBr (4)	pulsed-valve	0.5 ± 0.2	

[a] Determined per loss of reactant molecule (see text). [b] Given for the 1 mm orifice.

Reactivity of $ClNO_2$. N_2O_5 reacts with chloride according to reaction 1, producing $ClNO_2$ which is stable with respect to NaCl and therefore easily observable under our experimental conditions.[1] However, $ClNO_2$ does react with bromide according to reaction 4. This reaction may have implications for atmospheric chemistry and in addition represents a second option for $BrNO_2$ production in the laboratory.

$ClNO_2$ + KNO_2. Steady-state experiments of the interaction of $ClNO_2$ with KNO_2 powder substrates have been performed using MS detection at *m*/*e* 49 for $ClNO_2$ and LIF detection for NO_2. An average initial uptake coefficient of $\gamma = (1.7 \pm 0.2) \times 10^{-2}$ has been measured. No HONO formation (*m*/*e* 47) has been observed indicating the absence of HNO_3 which could have reacted with KNO_2 and released HONO. We conclude that $ClNO_2$ did not undergo hydrolysis under the present experimental conditions. The unique product detected in the gas phase was NO_2. The yield of NO_2 with respect to $ClNO_2$ consumed has been measured at 200% at the longest $ClNO_2$ residence time used (26 s). At decreasing $ClNO_2$ residence times, the NO_2 yield gradually decreased. The experimental results are summarized in Table 6 and reveal the occurrence of reaction 11:

$$ClNO_2 + KNO_2 \rightarrow KCl + 2\,NO_2 \qquad (11)$$

$ClNO_2$ + KBr: Product Analysis. The product analysis of steady-state experiments showed Br_2 as the only detectable product of reaction 4 with MS intensities at *m*/*e* 79, 81 and 158, 160 and 162 in agreement with the Br_2 mass spectrum. The mean Br_2 yield per molecule of $ClNO_2$ lost by uptake has been determined to be 0.55 ± 0.2 (see Table 7). An example of a steady-state experiment performed to measure the yield of Br_2 per loss of $ClNO_2$ is shown in Figure 7. During reference experiments in which KBr was exposed to a flow of Br_2, an interaction between Br_2 and KBr was measured which possibly may explain a yield of Br_2 less than unity.[15]

In real-time experiments we were able to detect MS signals at *m*/*e* 160, 79, and a weak contribution at *m*/*e* 93 and 95 (BrN^+) as product signals, along with the time-dependent disappearance of $ClNO_2$ monitored at *m*/*e* 46. We did not detect the fragment at *m*/*e* 97 corresponding to BrO^+. We were also able to rule out BrCl as a product of the reaction of $ClNO_2$ with bromide under our conditions. A typical pulsed-valve experiment is displayed in Figure 8. Data analysis of pulsed-valve experiments allow the determination of the uptake coefficient by fitting the reactant pulse to an exponential decay and extracting the decay constant. The yield is evaluated by integrating the calibrated product pulse at mass *m*/*e* 160 and comparing this value to the difference between the calibrated integrated

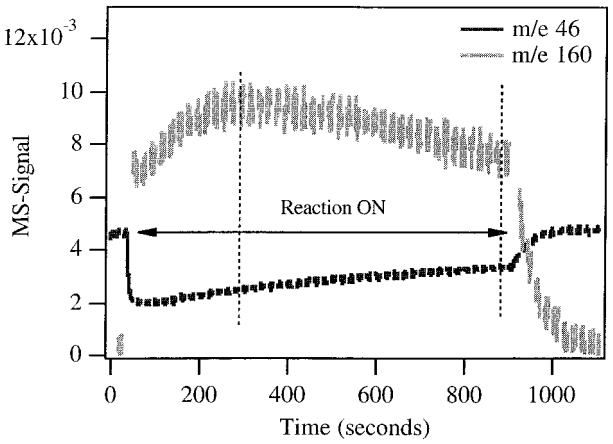

Figure 7. Steady-state experiment on reaction of $ClNO_2$ + KBr (reaction 4) using the 1 mm orifice and a continuous $ClNO_2$-flow rate of 2×10^{15} molecules s^{-1}. The sample (6 g of KBr powder) exposition begins at 50 s and ends at 900 s. The delay in the Br_2 signal rise (50 s < t < 250 s) is due to the filling time of the Knudsen cell. During the reaction, Br_2 was detected with a yield of 0.6 with respect to loss of $ClNO_2$, as integrated between the dotted lines.

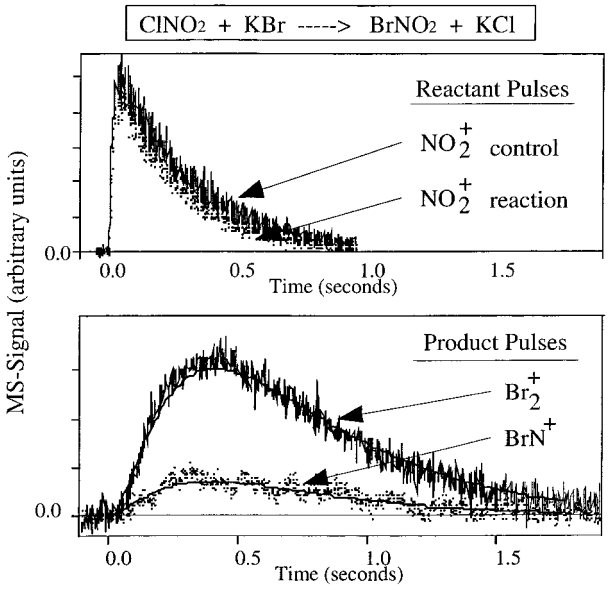

Figure 8. Pulsed-valve experiment of $ClNO_2$ on KBr (5 g of powder) performed using the 14 mm orifice. From this experiment we are able to measure the uptake coefficient by directly fitting the reactive $ClNO_2$ pulse to an exponential decay ($\gamma = 0.01$). The Br_2 yield per loss of $ClNO_2$ is determined to be 0.61 by comparing the integrals of the reactant and product signals. $BrNO_2$ is detected at mass *m*/*e* 93. The solid lines are fits obtained using a two-parameter model (see text).

nonreactive (sample absent) and reactive (sample present) reactant pulses monitored at mass *m*/*e* 46, corresponding to the amount of $ClNO_2$ lost per pulse.

We attribute the MS signal intensity at *m*/*e* 93 and 95 to $BrNO_2$. The product spectrum of this system is therefore consistent with the following mechanism:

$$ClNO_2 + KBr \rightarrow BrNO_2 + KCl \quad (4)$$

$$BrNO_2 + KBr \rightarrow Br_2 + KNO_2 \quad (3)$$

In additional experiments we confirmed that reaction 3 is fast and produces molecular bromine (see above).

In our first attempts to fit the pulsed-valve data for Figure 8, we used the simple two-step mechanism given by reactions 3 and 4. This reaction scheme led to a decay of $BrNO_2$, monitored at *m*/*e* 93, which was faster than experimentally observed in Figure 8. Therefore, we proposed a modification to the above reaction mechanism. Two reasons may be at the origin of this discrepancy: (1) $BrNO_2$ may remain adsorbed on the surface after its production, and its appearance in the gas phase is therefore delayed. This corresponds to the following mechanism:

$$ClNO_2(g) + KBr(s) \rightarrow BrNO_2(ads) + KCl(s) \quad (12)$$

$$BrNO_2(ads) \rightarrow BrNO_2(g) \quad (13)$$

$$BrNO_2(ads) + KBr(s) \rightarrow Br_2(g) + KNO_2(s) \quad (14)$$

(2) The reactive uptake of $ClNO_2$ is a two-step process, according to reactions 15 to (17):

$$ClNO_2(g) \rightarrow ClNO_2(ads) \quad (15)$$

$$ClNO_2(ads) + KBr(s) \rightarrow BrNO_2(g) + KCl(s) \quad (16)$$

$$BrNO_2(g) + KBr(s) \rightarrow Br_2(g) + KNO_2(s) \quad (17)$$

We are not able to distinguish between the two proposed mechanisms using the experimental results of the pulsed-valve experiments. However, it seems unlikely that the $ClNO_2$ uptake is a complex process, passing through an adsorbed state. The molecule diffuses into the internal void of the grain samples according to observation and theory (see below) which indicates that the lifetime of $ClNO_2$(ads) must be small relative to $1/k_{esc}$. This hypothesis is supported by surface residence time experiments of $ClNO_2$ on KBr where no measurable residence time has been observed.[16] In addition, Koch et al.[16] determined a residence time of $\tau = 0.7$ ms of $ClONO_2$ on NaCl which they explain by the interaction of the positively polarized Cl in $ClONO_2$ with Cl^- of the salt. Since bromine in $BrNO_2$ is also positively polarized, the adsorption of $BrNO_2$ on KBr resulting in a long-lived surface complex before reaction 14 may be possible. Therefore, the mechanism consisting of reactions 12−14 is not only consistent with residence time measurements[16] but may also explain the less than 100% yield of Br_2 observed in the gas-phase (Table 7) and the nonreactive uptake of $BrNO_2$ on KCl (see above). Consequently, the solid lines presented in Figure 8 have been obtained by using the mechanism involving the adsorption of $BrNO_2$ on the KBr powder corresponding to reactions 12−14. The rate-determining step in the mechanism given by reactions 12−14 is the desorption of $BrNO_2$ (reaction 13) with a rate constant $k_{13} = 3.1$ s^{-1} corresponding to a residence time on the salt of $\tau = 0.3$ s.

Kinetics of the Reaction. We have investigated the reactivity of the $ClNO_2$/KBr system as a function of reactant density and as a function of the surface presentation of the salt. We did not detect any systematic variation of the initial uptake as a function of the gas-phase density when the sample was presented as a powder. The uptake coefficient, $\gamma = (1.9 \pm 0.6) \times 10^{-2}$, measured on powders remained constant over the density range of 10^{10} to 10^{13} molecules cm^{-3}. Pulsed-valve experiments performed on powder surfaces also showed a similar uptake coefficient of $\gamma = (1.5 \pm 0.6) \times 10^{-2}$. The density independence of the measured initial uptake coefficient on one type of surface confirms that the process follows first-order kinetics.

To study the dependence of reaction 4 on the presentation of the reactive surface, we have performed uptake experiments on various types of substrate (powder, grain, spray-deposited salt

TABLE 8: Results Obtained for the Reaction of $ClNO_2$ + KBr as a Function of Surface Presentation

type of surface	number of experiments	measured uptake coefficient	corrected value of γ^a
spray	2	$(1.0 \pm 0.5) \times 10^{-4}$	
window-polished	1	$(1.5 \pm 1.0) \times 10^{-5}$	
window-depolished	1	$(1.0 \pm 0.5) \times 10^{-4}$	
powder	6	$(1.9 \pm 0.6) \times 10^{-2}$	1.0×10^{-4}
grain (350 μm)	19	$(1-100) \times 10^{-4}$	1.3×10^{-4}

[a] Corrections obtained by using the surface diffusion model described in ref 1.

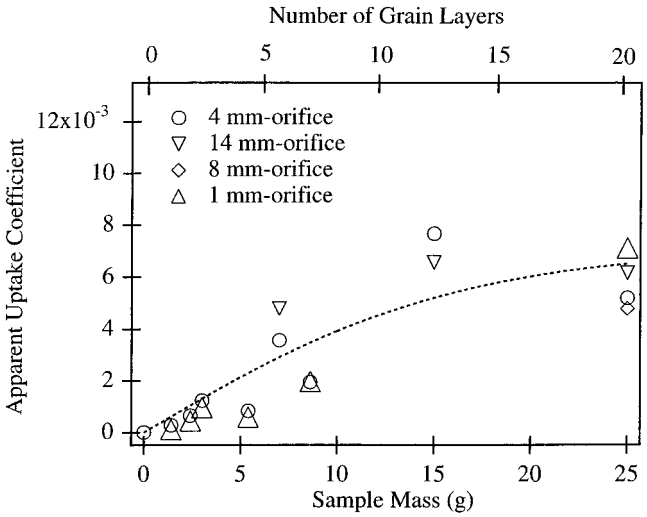

Figure 9. Results of monodisperse grain experiments (grain size 0.35 mm) using different orifice sizes. The dashed line is a fit obtained using the diffusion model proposed by Keyser and co-workers[13] using the value for the true uptake coefficient of 1.3×10^{-4}.

surfaces, and polished and depolished single-crystal optical flats). These experiments, summarized in Table 8, showed a strong variation of the measured uptake coefficient as a function of the surface presentation. In light of these results, we performed experiments using monodisperse grain samples of different mass in order to determine if the surface diffusion model of Keyser and co-workers[13] is applicable to the present case. Figure 9 displays the results obtained from these experiments. The dashed line is the best fit obtained using the surface diffusion model corresponding to $\gamma_{true} = 1.3 \times 10^{-4}$.

We note that the predicted value for the true uptake coefficient in the monodisperse grain experiments presented in Figure 9 ($\gamma_{true} = 1.3 \times 10^{-4}$) is in excellent agreement with the value measured on spray-deposited KBr samples and on *depolished* optical KBr flats. Powders are substrates composed of a great number of grain layers; for this type of sample the correction factor corresponds to the limit of a large number of layers and fortunately, in this limit, the correction factor becomes independent of the grain diameter. The diffusion model applied in this manner predicts a value of γ_{true} which is in excellent agreement with the results obtained on other KBr samples, namely, $\gamma_{true} = 1.0 \times 10^{-4}$, as shown in Table 8. The uptake coefficient of reaction 4 measured on *polished* KBr flats has been determined to be 1 order of magnitude smaller than the true uptake coefficient (γ_{true}) determined for all the other surfaces. We obtained a similar discrepancy for the case of N_2O_5 interacting with salt which was presented in previous work.[1] This discrepancy may perhaps be attributed to a change in crystallinity of the surface.

We have also carried out steady-state experiments on the interaction of $ClNO_2$ with bromide using NO_2-selective LIF detection. Indeed, NO_2 was observed, but the yield of NO_2 per $ClNO_2$ consumed was small, not exceeding 20% for the longest residence times, as summarized in Table 7. The appearance of NO_2 may be due to heterogeneous decomposition of $BrNO_2$ (reaction 8). In addition, in the fast secondary reaction of $BrNO_2$ with KBr (reaction 3), KNO_2 is formed, which may react with $ClNO_2$ according to reaction 11. The uptake coefficient of $ClNO_2$ on KNO_2 powder was found to be $\gamma = 2 \times 10^{-2}$ (see above), thus of the same magnitude as the uptake coefficient of $ClNO_2$ on KBr powder. Therefore it seems possible that at long residence times, when a sufficient amount of KNO_2 has been built up, $ClNO_2$ undergoes competitive reactions with KBr and KNO_2, both leading to a certain amount of NO_2 according to reactions 8 and 11, respectively. On the basis of our experiments, we may not distinguish one reaction channel from another. We therefore state that the observed NO_2 may be due to both reactions, namely, heterogeneous decomposition of $BrNO_2$ (reaction 8) and the reaction of $ClNO_2$ on KNO_2 (reaction 11) which has been formed in reaction 3.

Discussion

We have presented results on the reactivity of $ClNO_2$ and $BrNO_2$ toward various solid alkali salts. The reactions presented above have been studied in other laboratories using different techniques[5,8,17] which have been applied at higher pressures using aqueous solutions as a reactive surface.

George and co-workers[17] have shown that $ClNO_2$ reacts efficiently with halogen anions, notably with I^-; although their study was carried out involving the solution phase, the observed reactivity is analogous to our observations for reaction 4. Frenzel and co-workers have studied the same reactions as presented here on aqueous solutions using a wetted-wall flow tube experiment.[8] In general, our results agree well with the findings of Frenzel et al. in that Br_2 underwent a fast reaction with KNO_2 to form $BrNO_2$, and $ClNO_2$ reacted readily with Br^- solutions to produce $BrNO_2$. Hydrolysis of $ClNO_2$ and $BrNO_2$ was found to be slow. In agreement with our study, BrCl was not observed as a product of reaction 10. During the reaction of $ClNO_2$ with KNO_2, slow release of NO_2 into the gas phase has been observed.

However, there are two main discrepancies between the results of Frenzel et al.[8] and the ones presented in this work. They report that $BrNO_2$ has a lifetime that exceeds 1 h under their conditions.[18] This is in apparent contradiction to our results which show a lifetime of $BrNO_2$ in our reactor on the order of 10 s. The heterogeneous decomposition (reaction 8) is surprisingly rapid, which indicates that the process may take place on some uncoated parts of the Teflon-coated walls of our low-pressure reactor by virtue of its large surface area (Table 1). A semiquantitative RRK calculation using the dissociation energy determined by Kreutter et al. indicates that at the temperature and total pressures used in this study, the unimolecular decomposition of the $BrNO_2$ molecule should still be far in the falloff region, predicting a much longer lifetime with respect to only gas-phase decomposition.[9] This highlights a fundamental limitation of the Knudsen-cell technique: when working with compounds that are only marginally stable in the presence of surfaces, the loss to the walls may become a dominating effect because of the efficiency of the gas−wall interaction.

Recent calculations by Lee[19] show the existence of three different $BrNO_2$ isomers, trans-BrONO, cis-BrONO, and $BrNO_2$. The most stable isomer, $BrNO_2$, has a calculated room-temperature bond dissociation energy of 94.1 kJ mole^{-1}, whereas cis-BrONO has a bond dissociation energy of 67.4 kJ mole^{-1}.

TABLE 9: Summary of Reactions Studied in This Work

reaction	γ	$\Delta H_r^0{}_{298}$[a]	$\Delta H_r^0{}_{298}$[b]
$ClNO_2 + KCl \rightarrow Cl_2 + KNO_2$	no uptake	54.3 (50.1)	
$ClNO_2 + KBr \rightarrow BrCl + KNO_2$	no uptake	26.0 (19.1)	
$BrNO_2 + KCl \rightarrow ClNO_2 + KBr$ (10a)	no uptake	4.9 (7.6)	−15.6 (−12.9)
$BrNO_2 + KCl \rightarrow BrCl + KNO_2$ (10b)	no uptake	30.9 (26.7)	10.4 (6.2)
$ClNO_2 + KBr \rightarrow BrNO_2 + KCl$ (4)	1.3×10^{-4}	−4.9 (−7.6)	15.6 (12.9)
$BrNO_2 + KBr \rightarrow Br_2 + KNO_2$ (3)	>0.3	4.3 (−2.6)	−16.2 (−23.1)
$ClNO_2 + KNO_2 \rightarrow KCl + 2NO_2$ (11)	3.0×10^{-4}	−13.1 (−8.9)	
$BrNO_2 + KNO_2 \rightarrow KBr + 2NO_2$ (9)	no uptake	−8.2 (−1.3)	−28.7 (−21.8)
$BrNO_2 \rightarrow 0.5\ Br_2 + NO_2$ (8)		−2.0	−22.5

[a] Standard heats of reaction in kJ/mol for salt in the pure crystalline state and in aqueous solution at infinite dilution (values in brackets), using $\Delta H_f^0(BrNO_2) = 50.6$ kJ/mol from ref 19. [b] Same as footnote *a*, using $\Delta H_f^0(BrNO_2) = 71.1$ kJ/mol from ref 8.

Therefore, one additional possibility to explain the difference in the lifetime of $BrNO_2$ measured in our and in Zetzsch's laboratory may be due to the production of a different isomer as a primary product. Reactions 2, 4, and 6 may generate the less stable cis-BrONO as the initial product, which decomposes rapidly on our reactor walls, but isomerizes to $BrNO_2$ under high-pressure conditions used by Frenzel et al.[8] However, this hypothesis seems unlikely because only BrN^+ fragments but no BrO^+ fragments, the latter indicating the presence of BrONO, were observed in our product spectrum of reaction 6 not withstanding the fact that isomerization of an unstable form of $BrNO_2$ may be even faster on a solid substrate.

A second difference between our results and the results of Frenzel et al. is the reactivity of $BrNO_2$ toward chloride.[8] They found that reaction 4 is reversible in solution and that the equilibrium between $ClNO_2$ and $BrNO_2$ is established. This is in disagreement with our results where reaction between $BrNO_2$ and NaCl as well as on KCl has not been observed. The lack of reactivity is in agreement with the endothermicity of the elementary reaction 10a when the calculated standard heat of formation for $BrNO_2$ calculated by Lee[19] is used (Table 9). However, Frenzel et al. conceded that the interconversion reaction may not be a direct halogen exchange but may proceed via a complex reaction sequence involving Br_2 and BrCl.

In summary, we have studied the heterogeneous reactions of $ClNO_2$ and $BrNO_2$ with KCl, KBr, and KNO_2 and have found them to be in agreement with the standard heats of reaction $\Delta H_r^0{}_{298}$ as displayed in Table 9, as expected. Column three of Table 9 displays the thermochemistry using the calculated standard heat of formation of $BrNO_2$[19] [$\Delta H_f^0(BrNO_2)$] whereas column four uses the value reported by Kreutter et al.[9] which probably addresses the species BrONO rather than $BrNO_2$ as discussed by Frenzel et al.[8] Owing to our inability to observe reaction 10a, we support the lower value of $\Delta H_f^0(BrNO_2)$ calculated by Lee in agreement with the conclusions reached by Frenzel et al. This is displayed in Table 9 where the lower value of $\Delta H_f^0(BrNO_2)$ leads to a positive heat of reaction as opposed to a negative one when the higher value for $\Delta H_f^0(BrNO_2)$ is used. The identical argument also applies to reaction 4 which is the inverse of reaction 10a and which has been observed to occur under our conditions. The values for the heats of reaction depend somewhat on whether one uses the standard heats of formation for the salts in their pure crystalline state or as aqueous solutions at infinite dilution. We prefer at this point the solution values because they make reaction 3 slightly exothermic in relation to the values for the salts in their solid crystalline state. The solution values correspond more closely to the concept of the quasi-liquid state of the interface even though one has to exercize caution as the liquid layer is certainly highly concentrated. However, when one chooses to use standard heats of formation of concentrated aqueous salt solutions, the values for $\Delta H_r^0{}_{298}$ change by approximately 1 kJ/mol which is hardly of significance. In addition, an uncertainty in the calculated value of $\Delta H_f^0(BrNO_2)$ may invalidate the preference for the standard state of salts in their aqueous solution.

The difference in the reactivity of the two molecules, $BrNO_2$ and $ClNO_2$, may be rationalized by considering the difference in the oxidation state of the halogen atom, Br being in the oxidation state (+1) whereas Cl is formally in the (−1) state. Experimental evidence from this study supporting this hypothesis includes (1) the relative instability of $BrNO_2$ in the presence of bromide, and (2) the observed hydrolysis products: $ClNO_2$ is known to be the mixed anhydride of nitric and hydrochloric acid,[20] whereas $BrNO_2$ hydrolyzes to HOBr and HONO. HONO has been unambiguously observed in reaction 6 as well as reaction 2.[1] The fact that hydrolysis has not been observed in the reaction of $BrNO_2$ with KCl (NaCl) (reaction 10) and on $NaNO_3$ may be due to HONO yields below our detection limit. As stated above, the hydrolysis of $BrNO_2$ is a slow process, only 10% of the $BrNO_2$ is undergoing hydrolysis on KNO_2. Considering the hygroscopic nature of KNO_2, the hydrolysis of $BrNO_2$ may be faster on KNO_2 compared to NaCl and $NaNO_3$.

Atmospheric Implications. Reactions 1 and 2 generate photolyzable halogen-containing species which will ultimately lead to the release of active halogen into the atmosphere. The study shows that if $ClNO_2$ is produced in the presence of bromide, it can be converted to $BrNO_2$, even if sea-salt aerosol exists in a solid, albeit humid state. During the day $ClNO_2$ is mainly removed by photolysis; the photolysis rate constant $k_p = 1.6 \times 10^{-4}$ s^{-1} [21,22] is several orders of magnitude higher than the heterogeneous removal rate constant. However, at night, heterogeneous reactions may represent an efficient sink for $ClNO_2$. Any $BrNO_2$ that is released as a result of a heterogeneous reaction represents a source of photolyzable bromine. The flux of photolyzable bromine from the sea-salt aerosol may even be further enhanced if $BrNO_2$ reacts with available bromide to form Br_2. Atmospheric modeling studies are currently under way to assess the impact of these heterogeneous halogen sources on the tropospheric chemistry within the marine boundary layer.

Because we carry out our experiments at very low total pressures, thus at low partial pressures of water vapor, it is necessary to comment on the role of humidity. In fact, because the kinetics of water exchange with salt substrates at low pressures is inefficient,[23] our substrates may retain significant quantities of adsorbed water. Recent experiments performed by Finlayson-Pitts and co-workers have shown that adsorbed water plays a critical role in relation to interfacial chemistry on salt surfaces.[24,25] These studies point toward the existence of a so-called quasi-liquid layer of concentrated salt solution, and they suggest that the observed heterogeneous reactions take place on or within a thin film of solution even on nominally

dry salt substrates. We have evidence that this layer is preserved for many days even under our low-pressure conditions. For example, when we heat a "dry" spray-deposited salt film in our Knudsen reactor to 700 K, the integrated water flux from the sample corresponds to tens of formal monolayers of surface-adsorbed water.[23] We never observed any influence of the amount of water adsorbed on the salt surface on our initial uptake coefficients. However, we observed the effect of adsorbed water on the product formation: $BrNO_2$ undergoes hydrolysis on salt, forming HONO, and upon drying the salt, the HONO yield may be reduced. Thus it seems that water is not the limiting reagent and is abundantly available to form localized regions of concentrated salt solutions upon or within which interfacial reactions may take place.

Note Added in Proof. S. Fickert, F. Helleis, J. Adams, G. K. Moortgat, and J. N. Crowley in their paper "Reactive Uptake of $ClNO_2$ on Aqueous Bromide Solutions", submitted to this Journal, reach similar conclusions resulting from the interaction of $ClNO_2$ with aqueous solutions of bromide.

Acknowledgment. This work was funded by a contract from the Office Fédéral de l'Education et de la Science (OFES) as part of the SALT project carried out in the framework of the EU Environment and Climate Program. We thank Professor H. van den Bergh for fruitful discussions as well as for his lively interest and support.

References and Notes

(1) Fenter, F. F.; Caloz, F.; Rossi, M. J. *J. Phys. Chem.* **1996**, *100*, 1008.
(2) Livingston, F. E.; Finlayson-Pitts, B. J. *Geophys. Res. Lett.* **1991**, *18*, 17.
(3) Leu, M. T.; Timonen, R. S.; Keyser, L. F.; Yung, Y. L. *J. Phys. Chem.* **1995**, *99*, (9), 13203.
(4) Laux, J. M.; Hemminger, J. C.; Finlayson-Pitts, B. J. *Geophys. Res. Lett.* **1994**, *21*, 1623.
(5) Behnke, W.; Scheer, V.; Zetzsch, C. *J. Aerosol Sci.* **1993**, *S24*, S115.
(6) George, Ch.; Ponche, J. L.; Mirabel, P.; Behnke, W.; Scheer, V.; Zetzsch, C. *J. Phys. Chem.* **1994**, *98*, 8780.
(7) Behnke, W.; George, Ch.; Scheer, V.; Zetzsch, C. *J. Geophys. Res.* **1997**, *102*, 3795.
(8) Frenzel, A.; Scheer, V.; Sikorski, R.; George, Ch.; Behnke, W.; Zetzsch, C. *J. Phys. Chem. A* **1998**, *102*, 1329.
(9) Kreutter, K. D.; Nicovich, J. M.; Wine, P. H. *J. Phys. Chem.* **1991**, *95*, 4020.
(10) Fenter, F. F.; Caloz, F.; Rossi, M. J. *Rev. Sci. Instrum.* **1997**, *68*, 3180.
(11) Caloz, F.; Fenter, F. F.; Tabor, K. D.; Rossi, M. J. *Rev. Sci. Instrum.* **1997**, *68*, 3172.
(12) Ganske, J. A.; Berko, H. N.; Finlayson-Pitts, B. J. *J. Geophys. Res.* **1992**, *97* (D7), 7651.
(13) Keyser, L. F.; Moore, S. B.; Leu, M.-T. *J. Phys. Chem.* **1991**, *95*, 5496.
(14) Caloz, F.; Fenter, F. F.; Rossi, M. J. *J. Phys. Chem.* **1996**, *100*, 7494.
(15) Mochida, M.; Akimoto, H.; van den Bergh, H.; Rossi, M. J. *J. Phys. Chem.* **1998**, *102*, 4819.
(16) Koch, T.; Rossi, M. J. *J. Phys. Chem.* **1998**, submitted.
(17) George, C.; Behnke, W.; Scheer, V.; Zetzsch, C.; Magi, L.; Ponche, J. L.; Mirabel, P. *Geophys. Res. Lett.* **1995**, *22*, 1505.
(18) Scheffler, D.; Grothe, H.; Willner, H.; Frenzel, A.; Zetzsch, C. *Inorg. Chem.* **1997**, *36* (6), 335.
(19) Lee, T. J. *J. Phys. Chem.* **1996**, *100*, 19847.
(20) Hollemann A. F.; Wiberg, E. *Lehrbuch der Anorganischen Chemie*; de Gruyter: Berlin, **1985**; p. 605.
(21) Atkinson, R., et al. *J. Phys. Chem. Ref. Data* **1992**, *21* (6).
(22) Finlayson-Pitts, B. J.; Pitts, J. N. *Atmospheric Chemistry*; John Wiley & Sons: New York, **1986**.
(23) Caloz, F. Thesis No. 1628, Swiss Federal Institute of Technology (EPFL), 1997.
(24) Beichert, P.; Finlayson-Pitts, B. J. *J. Phys. Chem.* **1996**, *100*, 15218.
(25) Allen, H. C.; Laux, J. M.; Vogt, R.; Finlayson-Pitts, B. J.; Hemminger, J. C. *J. Phys. Chem.* **1996**, *100*, 6371.
(26) Seisel, S.; Caloz, F.; Fenter, F. F.; van den Bergh, H.; Rossi, M. J. *Geophys. Res. Lett.* **1997**, *24* (22), 2757.